General intelligence is associated with working memory-related functional connectivity change: evidence from a large sample study

Hikaru Takeuchi[a], Yasuyuki Taki[a,b,c], Rui Nouchi[d,e,f], Ryoichi Yokoyama[g], Yuka Kotozaki[h], Seishu Nakagawa[i,j], Atsushi Sekiguchi[b,k], Kunio Iizuka[l], Sugiko Hanawa[i], Tsuyoshi Araki[f], Carlos Makoto Miyauchi[i], Kohei Sakaki[j], Yuko Sassa[a], Takayuki Nozawa[m], Shigeyuki Ikeda[n], Susumu Yokota[o], Daniele Magistro[p], Ryuta Kawashima[a,f,n]

[a]*Division of Developmental Cognitive Neuroscience, Institute of Development, Aging and Cancer, Tohoku University, Sendai, Japan*

[b]*Division of Medical Neuroimaging Analysis, Department of Community Medical Supports, Tohoku Medical Megabank Organization, Tohoku University, Sendai, Japan*

[c]*Department of Radiology and Nuclear Medicine, Institute of Development, Aging and Cancer, Tohoku University, Sendai, Japan*

[d]*Creative Interdisciplinary Research Division, Frontier Research Institute for Interdisciplinary Science, Tohoku University, Sendai, Japan*

[e]*Human and Social Response Research Division, International Research Institute of Disaster Science, Tohoku University, Sendai, Japan*

[f]*Advanced Brain Science, Institute of Development, Aging and Cancer, Tohoku University, Sendai, Japan*

[g]*School of Medicine, Kobe University, Kobe, Japan*

[h]*Division of Clinical research, Medical-Industry Translational Research Center, Fukushima Medical University School of Medicine, Fukushima, Japan*

[i]*Department of Human Brain Science, Institute of Development, Aging and Cancer, Tohoku University, Sendai, Japan*

[j]*Division of Psychiatry, Tohoku Medical and Pharmaceutical University, Sendai, Japan*

[k]*Department of Behavioral Medicine, National Institute of Mental Health, National Center of Neurology and Psychiatry, Tokyo, Japan*

[l]*Department of Psychiatry, Tohoku University Graduate School of Medicine, Sendai, Japan*

[m] *Research Center for the Earth Inclusive Sensing Empathizing with Silent Voices, Tokyo Institute of Technology, Tokyo, Japan*

[n] *Department of Ubiquitous Sensing, Institute of Development, Aging and Cancer, Tohoku University, Sendai, Japan*

[o] *Faculty of Arts and Science, Kyushu University, Fukuoka, Japan*

[p] *Department of Sport Science, School of Science and Technology, Nottingham Trent University, Nottingham, UK*

Corresponding author:

Hikaru Takeuchi

Division of Developmental Cognitive Neuroscience, IDAC, Tohoku University

4-1 Seiryo-cho, Aoba-ku, Sendai 980-8575, Japan

Tel/Fax: +81-22-717-7988

E-mail: takehi@idac.tohoku.ac.jp

Keywords:

intelligence; Working memory; functional connectivity; N-back task; psychophysiological interaction

Short title: Association between intelligence and functional connectivity

Abstract

Background/Purpose: Psychometric intelligence is closely related to working memory (WM) and the associated brain activity. We aimed to clarify the associations between psychometric intelligence and WM-induced functional connectivity changes.

Methods: Here we determined the associations between psychometric intelligence measured by non-verbal reasoning (using the Raven's Advanced Progressive Matrix) and WM-induced changes in functional connectivity during the N-back paradigm, in a large cohort of 1221 young adults.

Results: We observed that the measures of general intelligence showed a significant positive correlation with WM-induced changes in the functional connectivity with the key nodes of the fronto-parietal network, such as the bilateral premotor cortices and the pre-SMA. Those

significant correlations were observed for (a) areas showing a WM-induced increase of the functional connectivity with the abovementioned key nodes, such as the lateral parietal cortex, (b) areas showing a WM-induced decrease of the functional connectivity with the abovementioned key nodes, (b-1) such as left perisylvian areas and cuneus, the fusiform gyrus, and the lingual gyrus, which play key roles in language processing, (b-2) hippocampus, and parahippocampal gyrus, which play key roles in memory processing, and (b-3) the key node of the default mode network such as the medial prefrontal cortex as well as (c) the border areas between (a) and (b).
Conclusion: Psychometric intelligence is associated with WM-induced changes in functional connectivity, influencing the way in which WM key nodes dynamically modulate the interaction with other brain nodes in response to WM.

Impact Statement

Psychophysiological interaction analysis is an old, widely used method to detect functional connectivity changes between different areas in response to task conditions. However, the associations of these task-related functional connectivity changes with cognitive functions remain poorly substantiated. We examined the associations between psychometric intelligence and WM-induced changes in functional connectivity in a large cohort of young adults. We discovered psychometric intelligence is associated with WM-induced changes in functional connectivity with WM key nodes and other brain areas.

Introduction

Psychometric intelligence is associated with the performance of a wide range of cognitive academic and job-related tasks (Cattell 1971). Performance in non-verbal reasoning tasks constitutes a representative measure of psychometric intelligence, which is strongly correlated with the general intelligence factor associated with performance in a wide range of cognitive tasks (Cattell 1971). On the other hand, working memory (WM) refers to the limited-capacity storage system involved in the maintenance and manipulation of information over short periods of

time (Baddeley 2003). The WM span is also strongly correlated with general intelligence and with the performance on a wide range of tasks (Baddeley 2003; Engle et al. 1999).

The neural mechanisms underlying individual differences in psychometric and general intelligence have been investigated by numerous functional and structural studies (Jung and Haier 2007). Those studies suggest that not only the lateral prefrontal cortex regions, but also the network involving the fronto-parietal areas (fronto-parietal network) play a key role in psychometric intelligence (Basten et al. 2015). Studies using functional MRI have investigated the associations between psychometric intelligence and neural activation during the N-back WM paradigm (Takeuchi et al. 2018). We have previously investigated the associations between psychometric intelligence and brain activity during the N-back task, analyzing data from over 1200 subjects with robust voxel-by-voxel permutation-based statistics (Takeuchi et al. 2018). Our results revealed that subjects with greater cognitive ability generally have a lower brain response to task demand [i.e., a lower increase in the activation of the network that is activated during the task, and a lower task-induced deactivation of the network that is deactivated during the task (particularly in the default mode network [DMN], which consists of the medial prefrontal cortex [mPFC], medial parietal cortex, and other areas). Individuals with higher fluid intelligence scores have demonstrated greater WM-related activity in the pre-supplementary motor area (SMA), suggesting this area plays a unique role during WM. Among these findings, the associations between lower task-induced activation and greater intelligence is partly consistent with the neural efficiency theory, which suggests lower prefrontal activity during tasks of low to moderate difficuty (Neubauer and Fink 2009). However, it should be noted that multiple studies investigating children showed that greater cognitive competence (including psychometric intelligence) is associated with greater task-induced activation and deactivation during WM (Darki and Klingberg 2015; Rosenberg et al. 2020; Satterthwaite et al. 2013). Given that BOLD responses (task-induced activation and deactivation) become largeas children age (Satterthwaite et al. 2013), advanced neurocognitive development may be associated with a larger BOLD response and thus, the possible age-specificity of the associations between intelligence and BOLD response should be noted.

On the other hand, several studies have previously investigated the associations between functional connectivity and individual cognitive abilities, although these studies are mostly based on resting state functional connectivity (RSFC) analyses. For example, Song et al. (2008) revealed that individuals with higher psychometric intelligence scores show greater RSFC between DLPFC and other areas of the fronto-parietal network and lower RSFC between DLPFC and the key nodes of the DMN. Similar conclusions were reported in the more recent study of RSFC (Hilger et al. 2020). Other RSFC studies also reported the importance of the RSFC between the key nodes of the fronto-parietal network for psychometric intelligence (Langeslag et al. 2013; Thatcher et al. 2016). Numerous recent studies have reported that whole-brain network characteristics across resting or task sessions (profiles of connectivity between whole-brain nodes or networks) can accurately predict psychometric intelligence and WM performance; among them, connectivity involving the fronto-parietal network plays an important role in such predictions (Avery et al. 2020; Finn et al. 2015; Yamashita et al. 2018). Further, Greene et al. (2018) showed that these whole-brain network characteristics across task sessions can better predict individual cognitive abilities than those derived from resting state scanning sessions. Van Den Heuvel et al. also reported the associations between psychometric intelligence and greater efficiency of the functional network during rest (Van Den Heuvel et al. 2009), though this was not replicated in a larger sample size (Kruschwitz et al. 2018). On the other hand, another study showed that the multivariate pattern of voxel-wise dynamic, trial-to-trial, inter-areal functional connectivity (defined by the correlation strength between the activation of each area in response to each WM trial) among occipito-parietal nodes significantly predicted WM performance (Weber et al. 2017). Structural connectivity analyses using fractional anisotropy measure of diffusion tensor imaging (DTI) also revealed the importance of brain connectivity for intelligence (Schmithorst 2009).

Psychophysiological interaction analysis (PPI)(Friston et al. 1997) is an old, widely used method to detect functional connectivity changes between different areas in response to task conditions. Through this method, it has been shown that the increase of functional connectivity within the fronto-parietal network (which is activated during WM) in response to WM demands (Takeuchi et al. 2012). Furthermore, Nagel et al. (2011) investigated the

associations between this functional connectivity change, in response to WM load and WM task accuracy, although only a non-significant tendency was found. On the other hand, a difference on functional connectivity change in response to task demand, as analyzed by PPI, was found to be associated with aging, caudate dopamine D1 receptor density and autistic diseases (Nagel et al. 2011; Rieckmann et al. 2011; Simard et al. 2015), suggesting that PPI measures reflect meaningful individual differences.

To date, the associations between psychometric intelligence and WM-induced functional connectivity changes remains to be investigated. The abovementioned studies that used connectivity data from task sessions studied the correlation of brain activity between different brain regions during the task (i.e. they did not investigate the differences or changes in strength of connectivity between the different conditions) (Avery et al. 2020; Finn et al. 2015; Greene et al. 2018). Moreover, although we showed previously that individuals with high fluid intelligence scores showed greater brain activity in pre-SMAs, the interactions between this and other brain areas in individuals with high fluid intelligence scores remain unknown. The present study aimed to clarify these issues, analyzing the data of N-back fMRI tasks of the huge sample used in the previous study (Takeuchi et al. 2018).

We hypothesized that greater psychometric intelligence is associated with a greater WM-induced functional connectivity change between the nodes of the fronto-parietal network. This reasoning is based on the previous findings that showed a decrease of these functional connectivity changes was previously found to be associated with aging, and aging is associated with a reduction of fluid intelligence (Nagel et al. 2011).

Understanding the neural bases of individual intelligence is of great scientific and social interest and PPI analysis is a widely used method to investigate task-induced functional connectivity changes. Therefore, investigating the nature of this measure in terms of association of intelligence comprises an important topic.

Material and Methods

Subjects

The present study is part of an ongoing project investigating the associations among brain imaging, cognitive function, and aging. This study included relevant and reliable cognitive measures and imaging data from 1221 healthy right-handed individuals (700 males and 521 females). The present study investigated associations between psychometric intelligence and WM-induced functional connectivity changes through PPI analyses. Based on apparent abnormalities of the results of individual PPI analyses, 15 subjects were removed from the 1236 subjects whose data was used in our previous study that investigated the association between brain activity during N-back tasks and psychometric intelligence (Takeuchi et al. 2018).

The subjects' mean age was 20.7 years (standard deviation [SD], 1.8 years; age range, 18–27 years). For detailed information on the subjects and limitations imposed by the cohort selection, see the Supplemental Methods and Supplemental Discussion, respectively. Written informed consent was obtained from all the participants or their guardians. The study protocol was approved by the Ethics Committee of Tohoku University and performed in accordance with the tenets of the old Declaration of Helsinki (1991) as well as the newer Declaration of Helsinki (2013). This experiment's ID in UMIN is UMIN000028817.

Assessment of psychometric measures of general intelligence

The Raven's Advanced Progressive Matrix (RAPM)(Raven 1998), a measure of non-verbal reasoning considered as the most strongly correlated with general intelligence (Raven 1998), was used to assess psychometric intelligence. This test contains 36 non-verbal items, which require a fluid reasoning ability. Each item consists of a 3 × 3 matrix with a missing piece to be completed by selecting the best among eight alternatives. The test score, corresponding to the number of correct answers in 30 minutes, was used as an index of individual psychometric intelligence. The test was performed as described previously in a study by our group, using the same assessment methods (Takeuchi et al. 2015b). Total score is used in this study as is the cases with previous studies (Raven 1998).

fMRI task. fMRI was used to map brain activity during cognitive tasks. The descriptions of this task are reproduced from our previous study using the same methods (Takeuchi et al.

2015d). The N-back task, which is typically used for fMRI studies, was used with conditions of 0-back (simple cognitive processes) and 2-back (WM). A simple block design (each block lasting 20 s) and the N-back WM task (Callicott et al. 1999) were
used to map brain activity during WM. The N-back task was performed during fMRI scanning as described previously (Takeuchi et al. 2011a, 2011b; Takeuchi et al. 2014). See **Supplemental Methods** for more details. Sufficient practice was allowed to ensure that the subjects understood the tasks and the item updating strategy to remember two by two during the 2-back task (Takeuchi et al. 2012). Reaction time (RT) and accuracy on 0-back and 2-back tasks were used in the analyses.

Image acquisition. MRI data were acquired using a 3T Philips Achieva scanner. Forty-two transaxial gradient-echo images (echo time, 30 ms; flip angle, 90°; slice thickness, 3 mm; FOV, 192 mm; matrix, 64 × 64) covering the entire brain were acquired at a repetition time of 2.5 s using an echo-planar sequence. A total of 174 functional volumes were obtained for the N-back session. Diffusion-weighted data were acquired using a spin-echo echo-planar imaging sequence, as described previously (Takeuchi et al. 2015c). The fractional anisotropy (FA) and mean diffusivity (MD) maps were calculated from the acquired images (Takeuchi et al. 2011c) and used for preprocessing of BOLD images. The descriptions of this subsection are mostly reproduced from our previous study using the exact same methods (Takeuchi et al. 2015d).

Imaging data preprocessing

Preprocessing and analysis of functional connectivity data were performed using SPM8 implemented in Matlab. Here we provide a summary, while the full details and methodological considerations are provided in our previous study (Takeuchi et al. 2018)**.** Briefly, prior
to analysis, individual BOLD images were realigned and re-sliced to the mean BOLD image, which was then realigned to the mean b = 0 image, as described previously (Takeuchi et al. 2011b). As the mean b = 0 image was aligned with both FA image and MD map, the BOLD image, b = 0 image, FA image, and MD map were all aligned. Then BOLD images were slice timing corrected. Then, all images were normalized using a previously validated two-step “new segmentation” algorithm for diffusion images, and the previously validated diffeomorphic

anatomical registration through exponentiated lie algebra (DARTEL)-based registration (Takeuchi et al. 2013). The voxel size of normalized BOLD images was $3 \times 3 \times 3$ mm^3. The processed images were spatially smoothed with 8-mm FWHM. The descriptions in this subsection are mostly reproduced from our previous study using the exact same methods (Takeuchi et al. 2018).

The reasons for why BOLD images were registered to diffusion-weighted images instead of to T1 weighted structural images for normalization can be found in the **Supplemental Methods**.

PPI analysis. Psychophysiological interaction (PPI) analysis was performed using SPM8 (Friston et al. 1997), to identify individual WM-induced functional connectivity changes within the regions of interest (ROIs).

Prior to PPI analyses, individual functional activation analyses were performed.

Individual-level statistical analyses were performed using a general linear model. A design matrix was fitted to each participant with one regressor in each N-back task condition (i.e., 0- or 2-back) using a standard hemodynamic response function. The cue phases of the N-back task were modeled in the same manner, but were not analyzed further. Sx parameters obtained by rigid body correction of head motion were regressed through inclusion in the regression model. Low-frequency fluctuations were removed using a high-pass filter with a cutoff value of 128 seconds. Serial correlations in fMRI time series were accounted for using an autoregressive AR(1) model during classical parameter estimation, as implemented in SPM. The descriptions in this subsection are mostly reproduced from our previous study using the similar methods (Takeuchi et al. 2015d).

PPI analysis was performed using the SPM8, as described previously (Takeuchi et al. 2012). The following five regions were seed ROIs because of the described reasons. The areas of the bilateral premotor cortices and bilateral DLPFC were chosen because they comprise key prefrontal nodes of the areas critical for WM (Baddeley 2003). The selection of bilateral premotor cortices and the pre-SMA as seed ROIs were because these three areas showed the strongest peaks within the anterior brain area for the 2-back – 0-back contrast, which demonstrated that these nodes are important for the execution of the N-back task.

Callicott JH, Mattay VS, Bertolino A, Finn K, Coppola R, Frank JA, Goldberg TE, Weinberger DR. 1999. Physiological characteristics of capacity constraints in working memory as revealed by functional MRI. Cerebral Cortex. 9: 20-26.

Cattell RB. 1971. Abilities: Their structure, growth, and action. Boston: Houghton-Mifflin.

Cona G, Semenza C. 2017. Supplementary motor area as key structure for domain-general sequence processing: A unified account. Neurosci Biobehav Rev. 72: 28-42.

Danti S, Handjaras G, Cecchetti L, Beuzeron-Mangina H, Pietrini P, Ricciardi E. 2018. Different levels of visual perceptual skills are associated with specific modifications in functional connectivity and global efficiency. Int J Psychophysiol. 123: 127-135.

Darki F, Klingberg T. 2015. The role of fronto-parietal and fronto-striatal networks in the development of working memory: a longitudinal study. Cereb Cortex. 25: 1587-1595.

Engle RW, Kane MJ, Tuholski SW. 1999. Individual differences in working memory capacity and what they tell us about controlled attention, general fluid intelligence, and functions of the prefrontal cortex. In: Models of working memory: Mechanisms of active maintenance and executive control (Miyake A, Shah P, eds.), pp 102-134. Cambridge: Cambridge University Press.

Finn ES, Shen X, Scheinost D, Rosenberg MD, Huang J, Chun MM, Papademetris X, Constable RT. 2015. Functional connectome fingerprinting: identifying individuals using patterns of brain connectivity. Nat Neurosci. 18: 1664-1671.

Friston KJ, Buechel C, Fink GR, Morris J, Rolls E, Dolan RJ. 1997. Psychophysiological and modulatory interactions in neuroimaging. Neuroimage. 6: 218-229.

Fuster JM. 2006. The prefrontal cortex: Anatomy, physiology, and neuropsychology of the frontal lobe: Raven Press New York.

Greene AS, Gao S, Scheinost D, Constable RT. 2018. Task-induced brain state manipulation improves prediction of individual traits. Nat Commun. 9: 1-13.

Greicius MD, Supekar K, Menon V, Dougherty RF. 2009. Resting-state functional connectivity reflects structural connectivity in the default mode network. Cereb Cortex. 19: 72-78.

Hilger K, Fukushima M, Sporns O, Fiebach CJ. 2020. Temporal stability of functional brain modules associated with human intelligence. Hum Brain Mapp. 41: 362-372.

Jung RE, Haier RJ. 2007. The Parieto-Frontal Integration Theory (P-FIT) of intelligence: converging neuroimaging evidence. Behav Brain Sci. 30: 135-154.

Kruschwitz JD, Waller L, Daedelow L, Walter H, Veer IM. 2018. General, crystallized and fluid intelligence are not associated with functional global network efficiency: A replication study with the human connectome project 1200 data set. Neuroimage. 171: 323-331.

Langeslag SJ, Schmidt M, Ghassabian A, Jaddoe VW, Hofman A, van der Lugt A, Verhulst FC, Tiemeier H, White TJ. 2013. Functional connectivity between parietal and frontal brain regions and intelligence in young children: the Generation R study. Hum Brain Mapp. 34: 3299-3307.

Magistro D, Takeuchi H, Nejad KK, Taki Y, Sekiguchi A, Nouchi R, Kotozaki Y, Nakagawa S, Miyauchi CM, Iizuka K, Yokoyama R, Shinada T, Yamamoto Y, Hanawa S, Araki T, Hashizume H, Sassa Y, Kawashima R. 2015. The Relationship between Processing Speed and Regional White Matter Volume in Healthy Young People. PLoS ONE. 10: e0136386.

Murphy S, Norbury R, Godlewska B, Cowen P, Mannie Z, Harmer C, Munafo M. 2012. The effect of the serotonin transporter polymorphism (5-HTTLPR) on amygdala function: a meta-analysis. Mol Psychiatry. 18: 512-520.

Nachev P, Kennard C, Husain M. 2008. Functional role of the supplementary and pre-supplementary motor areas. Nature Reviews Neuroscience. 9: 856-869.

Nagel IE, Preuschhof C, Li S-C, Nyberg L, Bäckman L, Lindenberger U, Heekeren HR. 2011. Load modulation of BOLD response and connectivity predicts working memory performance in younger and older adults. J Cogn Neurosci. 23: 2030-2045.

Neubauer AC, Fink A. 2009. Intelligence and neural efficiency. Neurosci Biobehav Rev. 33: 1004-1023.

Owen AM, McMillan KM, Laird AR, Bullmore E. 2005a. N-back working memory paradigm: a meta-analysis of normative functional neuroimaging studies. Human Brain Mapping. 25: 46-59.

Owen AM, McMillan KM, Laird AR, Bullmore E. 2005b. N‐back working memory paradigm: A meta‐analysis of normative functional neuroimaging studies. Hum Brain Mapp. 25: 46-59.

Picard N, Strick PL. 1996. Motor areas of the medial wall: a review of their location and functional activation. Cereb Cortex. 6: 342-353.

Power JD, Barnes KA, Snyder AZ, Schlaggar BL, Petersen SE. 2012. Spurious but systematic correlations in functional connectivity MRI networks arise from subject motion. Neuroimage. 59: 2142-2154.

Price CJ. 2010. The anatomy of language: a review of 100 fMRI studies published in 2009. Ann N Y Acad Sci. 1191: 62-88.

Raven J. 1998. Manual for Raven's progressive matrices and vocabulary scales. Oxford: Oxford Psychologists Press.

Reuter-Lorenz PA, Jonides J, Smith EE, Hartley A, Miller A, Marshuetz C, Koeppe RA. 2000. Age differences in the frontal lateralization of verbal and spatial working memory revealed by PET. J Cogn Neurosci. 12: 174-187.

Rieckmann A, Karlsson S, Fischer H, Bäckman L. 2011. Caudate dopamine D1 receptor density is associated with individual differences in frontoparietal connectivity during working memory. J Neurosci. 31: 14284-14290.

Rosenberg MD, Martinez SA, Rapuano KM, Conley MI, Cohen AO, Cornejo MD, Hagler DJ, Jr., Meredith WJ, Anderson KM, Wager TD, Feczko E, Earl E, Fair DA, Barch DM, Watts R, Casey BJ. 2020. Behavioral and Neural Signatures of Working Memory in Childhood. J Neurosci. 40: 5090-5104.

Sambataro F, Murty VP, Callicott JH, Tan HY, Das S, Weinberger DR, Mattay VS. 2008. Age-related alterations in default mode network: Impact on working memory performance. Neurobiol Aging.

Satterthwaite TD, Wolf DH, Erus G, Ruparel K, Elliott MA, Gennatas ED, Hopson R, Jackson C, Prabhakaran K, Bilker WB. 2013. Functional maturation of the executive system during adolescence. J Neurosci. 33: 16249-16261.

Schilling C, Kühn S, Paus T, Romanowski A, Banaschewski T, Barbot A, Barker G, Brühl R, Büchel C, Conrod P. 2012. Cortical thickness of superior frontal cortex predicts impulsiveness and perceptual reasoning in adolescence. Mol Psychiatry. 18: 624-630.

Schmithorst VJ. 2009. Developmental sex differences in the relation of neuroanatomical connectivity to intelligence. Intelligence. 37: 164-173.

Seitz RJ, Nickel J, Azari NP. 2006. Functional modularity of the medial prefrontal cortex: involvement in human empathy. Neuropsychology. 20: 743.

Simard I, Luck D, Mottron L, Zeffiro TA, Soulières I. 2015. Autistic fluid intelligence: Increased reliance on visual functional connectivity with diminished modulation of coupling by task difficulty. NeuroImage: Clinical. 9: 467-478.

Smith SM, Nichols TE. 2009. Threshold-free cluster enhancement: addressing problems of smoothing, threshold dependence and localisation in cluster inference. NeuroImage. 44: 83-98.

Song M, Zhou Y, Li J, Liu Y, Tian L, Yu C, Jiang T. 2008. Brain spontaneous functional connectivity and intelligence. Neuroimage. 41: 1168-1176.

Takeuchi H, Sugiura M, Sassa Y, Sekiguchi A, Yomogida Y, Taki Y, Kawashima R. 2012. Neural correlates of the difference between working memory speed and simple sensorimotor speed: an fMRI study. PLoS ONE. 7: e30579.

Takeuchi H, Taki Y, Hashizume H, Sassa Y, Nagase T, Nouchi R, Kawashima R. 2011a. Effects of training of processing speed on neural systems. J Neurosci. 31: 12139-12148.

Takeuchi H, Taki Y, Hashizume H, Sassa Y, Nagase T, Nouchi R, Kawashima R. 2011b. Failing to deactivate: the association between brain activity during a working memory task and creativity. Neuroimage. 55: 681-687.

Takeuchi H, Taki Y, Nouchi R, Hashizume H, Sassa Y, Sekiguchi A, Kotozaki Y, Nakagawa S, Nagase T, Miyauchi M, C., Kawashima R. 2014. Associations among imaging measures (2): The association between gray matter concentration and task-induced activation changes. Hum Brain Mapp. 35: 185-198.

Takeuchi H, Taki Y, Nouchi R, Sekiguchi A, Hashizume H, Sassa Y, Kotozaki Y, Miyauchi CM, Yokoyama R, Iizuka K, Seishu N, Tomomi N, Kunitoki K, Kawashima R. 2015a. Degree centrality and fractional amplitude of low-frequency oscillations associated with Stroop interference. Neuroimage. 119: 197-209.

Takeuchi H, Taki Y, Nouchi R, Yokoyama R, Kotozaki Y, Nakagawa S, Sekiguchi A, Iizuka K, Hanawa S, Araki T, Miyauchi CM, Sakaki K, Sassa Y, Nozawa T, Ikeda S, Yokota S, Daniele M, Kawashima R. 2018. General intelligence is associated with working memory-related brain activity: new evidence from a large sample study. Brain Struct Funct. Epub ahead of print.

Takeuchi H, Taki Y, Nouchi R, Yokoyama R, Kotozaki Y, Nakagawa S, Sekiguchi A, Iizuka K, Yamamoto Y, Hanawa S, Araki T, Miyauchi M, Calros , Shinada T, Sakaki K, Sassa Y, Nozawa T, Ikeda S, Yokota S, Daniele M, Kawashima R. 2017. Global associations between regional gray matter volume and diverse complex cognitive functions: evidence from a large sample study. Scientific Reports. 7: article 10014.

Takeuchi H, Taki Y, Sassa Y, Hashizume H, Sekiguchi A, Fukushima A, Kawashima R. 2011c. Verbal working memory performance correlates with regional white matter structures in the fronto-parietal regions. Neuropsychologia. 49: 3466-3473

Takeuchi H, Taki Y, Sekiguchi A, Nouchi R, Kotozaki Y, Nakagawa S, Miyauchi CM, Iizuka K, Yokoyama R, Shinada T. 2015b. Amygdala and cingulate structure is associated with stereotype on sex-role. Scientific reports. 5: article 14220.

Takeuchi H, Taki Y, Sekuguchi A, Hashizume H, Nouchi R, Sassa Y, Kotozaki Y, Miyauchi CM, Yokoyama R, Iizuka K, Nakagawa S, Nagase T, Kunitoki K, Kawashima R. 2015c. Mean diffusivity of globus pallidus associated with verbal creativity measured by divergent thinking and creativity-related temperaments in young healthy adults. Hum Brain Mapp. 36: 1808-1827.

Takeuchi H, Taki Y, Thyreau B, Sassa Y, Hashizume H, Sekiguchi A, Nagase T, Nouchi R, Fukushima A, Kawashima R. 2013. White matter structures associated with empathizing and systemizing in young adults. Neuroimage. 77: 222-236.

Takeuchi H, Tomita H, Taki Y, Kikuchi Y, Ono C, Yu Z, Sekiguchi A, Nouchi R, Kotozaki Y, Nakagawa S. 2015d. Cognitive and neural correlates of the 5-repeat allele of the dopamine D4 receptor gene in a population lacking the 7-repeat allele. Neuroimage. 110: 124-135.

Thatcher R, Palmero-Soler E, North D, Biver C. 2016. Intelligence and eeg measures of information flow: efficiency and homeostatic neuroplasticity. Scientific reports. 6: 38890.

Van Den Heuvel MP, Stam CJ, Kahn RS, Pol HEH. 2009. Efficiency of functional brain networks and intellectual performance. J Neurosci. 29: 7619-7624.

Vul E, Harris C, Winkielman P, Pashler H. 2009. Reply to comments on “puzzlingly high correlations in fMRI studies of emotion, personality, and social cognition”. Perspect Psycholo Sci. 4: 319-324.

Wager TD, Davidson ML, Hughes BL, Lindquist MA, Ochsner KN. 2008. Prefrontal-subcortical pathways mediating successful emotion regulation. Neuron. 59: 1037-1050.

Weber EMG, Hahn T, Hilger K, Fiebach CJ. 2017. Distributed patterns of occipito-parietal functional connectivity predict the precision of visual working memory. Neuroimage. 146: 404-418.

Yamashita M, Yoshihara Y, Hashimoto R, Yahata N, Ichikawa N, Sakai Y, Yamada T, Matsukawa N, Okada G, Tanaka SC. 2018. A prediction model of working memory across health and psychiatric disease using whole-brain functional connectivity. Elife. 7: e38844.

Table 1. Brain regions showing significant correlations between WM-related increase of functional connectivity with the left premotor cortex and the RAPM score

Included gray matter areas* (number of significant voxels in the left and right sides of each anatomical area)	x	y	z	TFCE score	Corrected *P*-value (FWE, TFCE)	Cluster size (voxels)	Activated/ deactivated	Increase/ decrease of functional connectivity	r**
Caudate (L:24, R:17)/Anterior cingulum (L:137, R:105)/Middle cingulum (L:42, R:70)/Superior frontal medial area (L:228, R:119)/Superior frontal other areas (R:18)/	9	18	8	808.15	0.005	1024	476/487	321/664	0.143
Calcarine Cortex (L:208, R:192)/Cuneus (L:117, R:87)/Fusiform gyrus (L:12, R:15)/Heschl gyrus (R:3)/Hippocampus (L:59, R:57)/Insula (R:3)/Lingual gyrus (L:431, R:433)/Middle occipital lobe (L:3, R:7)/Superior occipital lobe (L:2)/Parahippocampal gyrus (L:93, R:76)/Precuneus (L:62, R:32)/Rolandic operculum (R:8)/Middle temporal gyrus (R:13)/Superior temporal gyrus (R:18)/Thalamus (R:4)/Thalamus (L:203, R:88)/	−12	−57	−9	782.16	0.005	2295	1222/746	180/1966	0.116
Middle frontal other areas (L:1)/Postcentral gyrus	−39	−18	36	627.59	0.010	136	48/69	19/107	0.103

(L:63)/Precentral gyrus (L:20)/									
Superior frontal medial area (L:4, R:7)/Superior frontal other areas (L:2, R:3)/Supplemental motor area (L:43, R:61)***/	−6	12	69	562.05	0.016	117	70/39	63/45	0.117
Middle cingulum (L:33, R:23)/	0	−24	36	549.30	0.018	59	0/59	0/59	0.107
Superior frontal medial area (L:1)/	−12	51	6	524.88	0.022	1	0/1	0/1	0.076

*Labelings of the anatomical regions of gray matter were based on the WFU PickAtlas Tool (http://www.fmri.wfubmc.edu/cms/software#PickAtlas/) (Maldjian et al. 2004; Maldjian et al. 2003) and on the PickAtlas automated anatomical labeling atlas option (Tzourio-Mazoyer et al. 2002). In this atlas, temporal pole areas and some other areas include all subregions. The superior frontal other areas include the areas in the superior frontal gyrus, other than the medial, orbital, and medial-orbital parts of the superior frontal gyrus.

** Simple correlation coefficients between mean beta estimates of significant clusters (mean values of the beta estimates of the target contrast of all voxels within the significant clusters) and RAPM score. Note that due to overfitting in whole-brain analyses (Vul et al. 2009), the correlation coefficients of significant areas are overestimated to a degree depeding on the sample size and number of comparisons.

*** This area is classified as the supplementary motor area in this atlas. However, as noted in the Results section, it has been pointed out this area mostly specifically corresponds to pre-supplementary motor area ((Picard and Strick 1996; Zilles et al. 1995), therefore, we called so in this table, too.

Table 2. Brain regions showing significant correlations between WM- related increase of the functional connectivity with right premotor cortex and The RAPM score.

Included gray matter areas* (number of significant voxels in the left and right sides of each anatomical area)	x	y	z	TFCE score	Corrected *P*-value (FWE, TFCE)	Cluster size (voxels)	Activated/ deactivated	Increase/ decrease of functional connectivity	r**
Inferior frontal orbital area (L:8)/Heschl gyrus (L:3)/Hippocampus (L:10)/Insula (L:134)/Putamen (L:2)/Middle temporal gyrus (L:6)/Superior temporal gyrus (L:113)/	−42	−3	−6	645.41	0.011	293	28/253	0/293	0.114
Angular gyrus (L:3)/Inferior parietal lobule (L:20)/Rolandic operculum (L:2)/Supramarginal gyrus (L:64)/Middle temporal gyrus (L:5)/Superior temporal gyrus (L:23)/	−39	−42	18	643.30	0.011	164	99/41	69/63	0.125
Fusiform gyrus (L:9)/Hippocampus (L:39)/Lingual gyrus (L:103)/Parahippocampal gyrus (L:47)/Precuneus (L:10)/Cerebellum	−12	−39	−9	619.15	0.014	274	96/128	14/237	0.116

(L:52)/

*Labelings of the anatomical regions of gray matter were based on the WFU PickAtlas Tool (http://www.fmri.wfubmc.edu/cms/software#PickAtlas/) (Maldjian et al. 2004; Maldjian et al. 2003) and on the PickAtlas automated anatomical labeling atlas option (Tzourio-Mazoyer et al. 2002). In this atlas, temporal pole areas and some other areas include all subregions. The superior frontal other areas include areas in the superior frontal gyrus, other than the medial, orbital, and medial-orbital parts of the superior frontal gyrus.

Table 3. Brain regions Showing significant correlations between WM-related increase of the functional connectivity with the pre-supplementary motor cortex and the RAPM score.

Included gray matter areas* (number of significant voxels in the left and right sides of each anatomical area)	x	y	z	TFCE score	Corrected *P*-value (FWE, TFCE)	Cluster size (voxels)	Activated/ Deactivated areas (voxels)	Areas of Increase/ decrease of functional connectivity (voxels)	r**
Anterior cingulum (L:10, R:5)/Superior frontal medial area (L:222, R:120)/Superior frontal other areas (L:9, R:22)/Supplemental motor area (L:29, R:18)/	6	45	41	676,77	0.009	401	15/382	7/393	0.129

*Labelings of the anatomical regions of gray matter were based on the WFU PickAtlas Tool (http://www.fmri.wfubmc.edu/cms/software#PickAtlas/) (Maldjian et al. 2004; Maldjian et al. 2003) and on the PickAtlas automated anatomical labeling atlas option (Tzourio-Mazoyer et al. 2002). In this atlas, temporal pole areas and some other areas include all subregions. The superior frontal other areas include areas in the superior frontal gyrus, other than the medial, orbital, and medial-orbital parts of the superior frontal gyrus.

Figure legends

Figure 1. Regions activated or deactivated and showing increased or decreased functional connectivity with the seed ROIs. [a,b,c] Regions specifically activated (red) and deactivated (green or blue) in response to WM demand (2-back–0-back) are displayed at a height threshold of 0.05, corrected for FDR. [d,e,f] Regions specifically showing increase (red) and decrease (green or blue) of the functional connectivity with the left premotor cortex in response to WM demand (2-back–0-back) are displayed at a height threshold of 0.05, corrected for FDR. [g,h,i] Regions specifically showing increase (red) and decrease of the functional connectivity with the right premotor cortex (green or blue) in response to WM demand (2-back–0-back) are displayed at a height threshold of 0.05, corrected for FDR. [j,k,l] Regions specifically showing increase (red) and decrease of the functional connectivity with the pre-supplementary motor area (green or blue) in response to WM demand (2-back–0-back) are displayed at a height threshold of 0.05, corrected for FDR. The right figures represent the results of average of all the samples. [a,d,g,j] Results are presented on a "render" image of SPM8. [b,c,e,f,h,i,k,l] Results are overlaid on a "single-subject T1" SPM8 image.

Figure 2. Brain regions showing significant correlations between WM-related increase of the functional connectivity with the left premotor cortex and the RAPM score. RAPM score and specific changes of the functional connectivity with the left premotor cortex in response to WM demand (2-back–0-back) showed significant positive correlations in (a, b) the anterior medial parts of the brain (ACC, MCC, mPFC), (e,f) the posterior parts of the brain (bilateral calcarine cortex, cuneus, hippocampus, lingual gyrus, parahippocampal gyrus, precuneus, thalamus), (i,j) the areas of the middle cingulate gyrus (m, n) and the areas of the left precentral and postcentral gyrus. (a, e, i, m) The scatter plots present the associations between the psychometric scores and the mean beta estimates of significant clusters (mean values of the beta estimates of the target contrast of all voxels within the significant clusters). (b, f, j, n) Areas of significant correlations. The results were obtained using a threshold of $P < 0.025$, corrected for multiple comparisons based on 5000 permutations using the TFCE scores. The color bars reflect the TFCE scores. All results are overlaid on a "single-subject T1" SPM8 image. (c, d, g, h, k, l, o, p) Regions specifically showing increase (red) and decrease (blue) of the functional connectivity with the left premotor cortex in response to WM demand (2-back–0-back) are displayed at a height threshold of 0.05, corrected for

FDR in the corresponding regions (b, f, j, n). The right panels represent the results of average functional connectivity of all the samples. And note even if the group average show robust increases of functional connectivity, there can be individual substantial variations and some subjects can show reliable decreases as pointed out in the previous studies (Gordon et al. 2017). Color bars represent T scores. All results are overlaid on a "single-subject T1" SPM8 image.

Figure 3. Brain regions showing significant correlations between WM-related increase of the functional connectivity with the right premotor cortex and the RAPM score. The RAPM score and change of the functional connectivity with the right premotor cortex in response to WM demand (2-back–0-back) showed significant positive correlations in (a, b) the left insula, the left superior temporal gyrus, and (e,f) areas around the left inferior parietal lobule, the left supramarginal gyrus and, the left superior temporal gyrus. (a, e) The scatter plots present the associations between the psychometric scores and the mean beta estimates of significant clusters (mean values of the beta estimates of the target contrast of all voxels within the significant clusters). (b, f) Areas of significant correlations. The results were obtained using a threshold of $P < 0.025$, corrected for multiple comparisons based on 5000 permutations using the TFCE scores. The color bars represent the TFCE scores. All results are overlaid on a "single-subject T1" SPM8 image. (c, d, g, h) Regions specifically showing an increase (red) and decrease (blue) of the functional connectivity with the right premotor cortex in response to WM demand (2-back–0-back) are displayed at a height threshold of 0.05, corrected for FDR in corresponding regions (b, f). The right panels represent the results of average functional connectivity of all the samples. And note even if the group average show robust increases of functional connectivity, there can be individual substantial variations and some subjects can show reliable decreases as pointed out in the previous studies (Gordon et al. 2017). Color bars reflect T scores. All results are overlaid on a "single-subject T1" SPM8 image.

Figure 4. Brain regions showing significant correlations between WM-related increase of the functional connectivity with the pre-supplementary motor cortex and the RAPM score. The RAPM score and change of the functional connectivity with the pre-supplementary motor area in response to WM demand (2-back–0-back) showed significant positive correlations in (a, b) the ACC, mPFC, pre-supplemental motor area. (a, e) The scatter plots represent the associations between the psychometric scores and the mean beta estimates of significant clusters (mean values of the beta

estimates of the target contrast of all voxels within the significant clusters). (bf) Areas of significant correlations. The results were obtained using a threshold of $P < 0.025$, corrected for multiple comparisons based on 5000 permutations using the TFCE scores. The color bars represent the TFCE scores. All results are overlaid on a “single-subject T1” SPM8 image. (c, d) Regions specifically showing an increase (red) and decrease (blue) of the functional connectivity with the left premotor cortex in response to WM demand (2-back–0-back) are displayed at a height threshold of 0.05, corrected for FDR in corresponding regions (b). The right panels represent the results of average functional connectivity of all the samples. And note even if the group average show robust increases of functional connectivity, there can be individual substantial variations and some subjects can show reliable decreases as pointed out in the previous studies (Gordon et al. 2017). Color bars represent the T scores. All results are overlaid on a “single-subject T1” SPM8 image.

Gordon EM, Laumann TO, Gilmore AW, Newbold DJ, Greene DJ, Berg JJ, Ortega M, Hoyt-Drazen C, Gratton C, Sun H. 2017. Precision functional mapping of individual human brains. Neuron. 95: 791-807. e797.

Figure 1

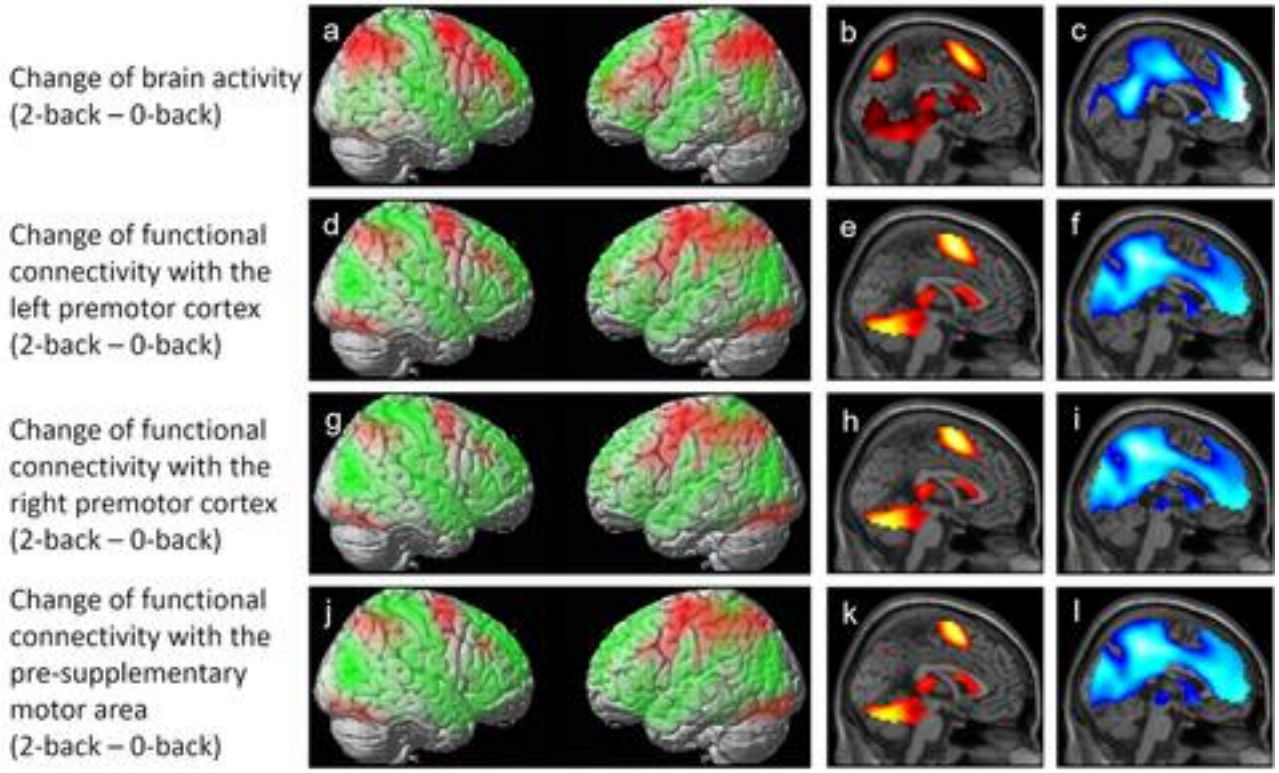

Figure 2

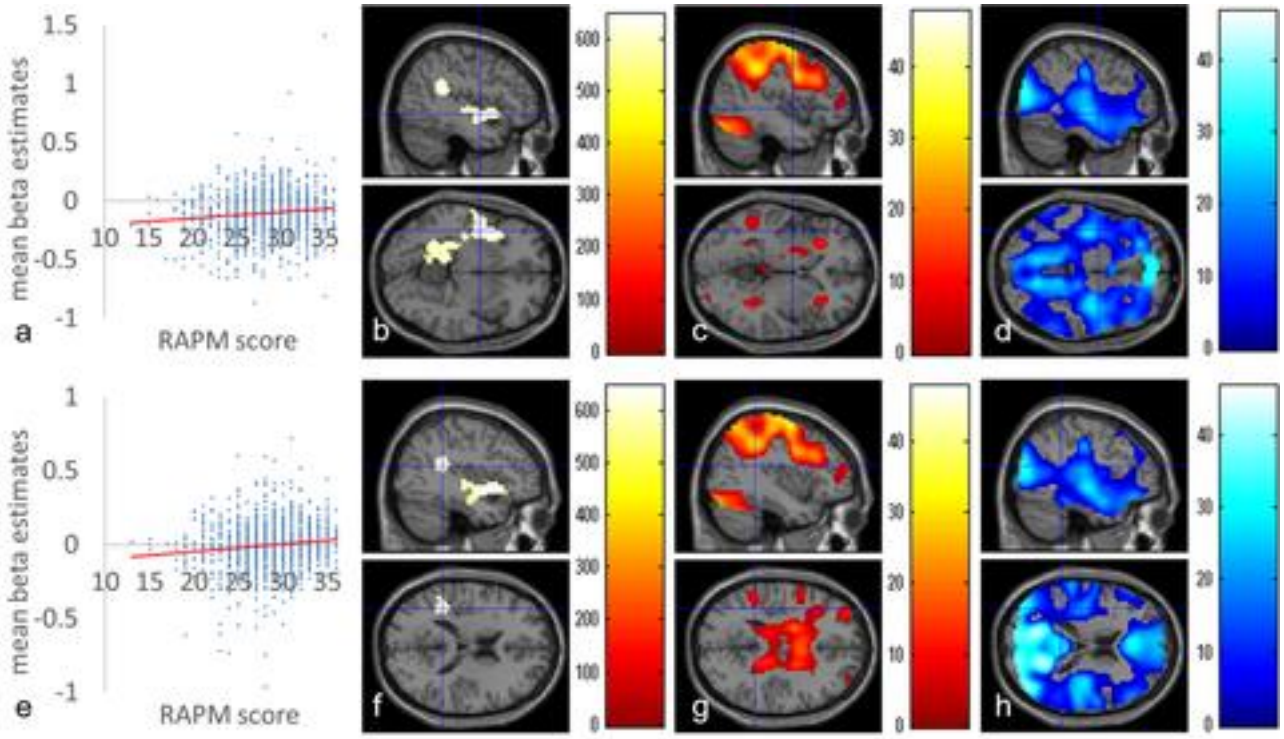

Figure 3

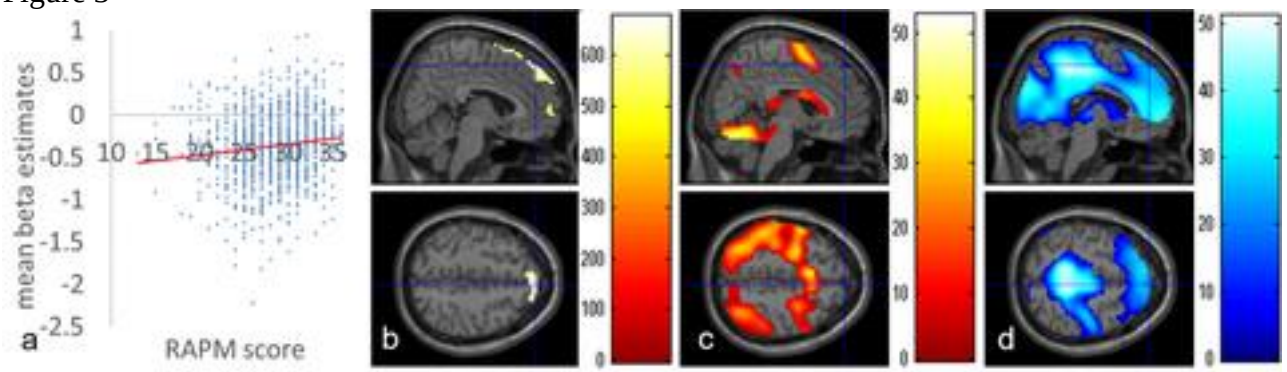

Figure 4